MATEC Web of Conferences **13**, 02001 (2014)
DOI: 10.1051/matecconf/ 20141302001

Effects of Capillary Pressure on Multiphase Flow during CO_2 Injection in Saline Aquifer

J.S. Pau[1,a], W.K.S. Pao[1,b], S.P. Yong[2,a] and P.Q. Memon[2,b]

[1]Universiti Teknologi PETRONAS Mechanical Department, 31750 Tronoh, Perak Darul Ridzuan, Malaysia
[2]Universiti Teknologi PETRONAS Computer and Information Science Department, 31750 Tronoh, Perak Darul Ridzuan, Malaysia

Abstract. This paper focused on supercritical CO_2 injection into saline aquifer, in particular its capillarity's effects on the plume migration, reservoir pressure alteration and CO_2 flux density. The numerical method used to solve the incompressible two-phase flow equations is based on the mimetic method, which conserves the mass and fluxes simultaneously. The investigation showed that exclusion of capillarity can greatly underestimate the CO_2 plume migration and resulted in distinctive reservoir pressure distribution. It is found that capillarity showed no significant effect on the flux intensity of CO_2.

1 Introduction

Reduction of CO_2 emission can be achieved through carbon capture and its subsequent geological storage (CCS) [1-3]. Saline aquifer has been the main focus of CCS due to its wide availability and potential storage capacity of 1000Gt [3]. This paper briefly discussed the two phase flow equation starting from the Darcy's law and limit the scope to horizontal two incompressible phases. The objective of current study is to study the effects of capillary pressure on the saturation migration, pressure and flux intensity of CO_2 after 300 days of injection.

2 Literature Reviews

2.1 CO_2 Sequestration in Geological Sites

CO_2 has been identified as the most important greenhouse gas (GHG) which is responsible for global warming [4]. Approximately 24Gt of CO_2 emitted from human activities annually, an amount that exceeds the capacity of natural systems to absorb them [5-6]. Carbon capture and geological storage is a promising technology that reduces GHG emission into the atmosphere [7-8], and one of the major potential geological storage is the saline aquifers [5,8]. According to [3], the estimated global storage

[a] jionseanpau@gmail.com
[b] william.paokings@petronas.com.my

potential in saline aquifer is 1000Gt, thus providing the most substantial carbon dioxide storage capacity [9-10].

2.2 Two-Phase Flow

The storage of CO_2 in sub- or supercritical state in geological media involves an active interaction amongst the solid matrix, country rock and two fluid phases [11]. Mass conservation equation (also known as the continuity equation) relates the pressure p and the total (interstitial) velocity, $\vec{v}$. We obtain a first-order elliptic system which describes the incompressible flow in porous media by combining the Darcy's law and mass-conservation equation [12].

$$\nabla \cdot \mathbf{v} = q, \quad \mathbf{v} = -\frac{\mathbf{K}}{\mu}\left(\nabla p + \rho g \nabla z\right) \tag{1}$$

where $\mathbf{v}$ is the vector representing Darcy velocity, ∇p is the pressure drop in the direction of flow, μ is the fluid viscosity and K denotes the permeability tensor. The capillary pressure, p_c, is related to saturation of wetting fluid, as written in mathematical equation,

$$p_c\left(S_w\right) = p_n - p_w \tag{2}$$

Assuming incompressible flow, a two phase system, with one wetting and another non-wetting phase can be described as,

$$\left.\begin{aligned} &\nabla \cdot \mathbf{v} = q, \quad \mathbf{v} = -\mathbf{K}\left(\lambda \nabla p + \left(\lambda_w \rho_w + \lambda_n \rho_n\right) g \nabla D\right) \\ &\phi \frac{\partial S_w}{\partial t} + \nabla \cdot \left(f_w \lambda_n \nabla p_c\right) + \nabla \cdot \left(f_w \mathbf{v}_t\right) = Q_w \end{aligned}\right\} \tag{3}$$

where, ρ_α represents the density of phase α , λ_α denotes the mobility of phase α and $f_w = \lambda_w / \lambda$ is the fractional flow term of wetting phase.

2.3 Discretization of Flow Equation

The notation used in this paragraph is in reference to [15]. According to [15], in the mimetic difference method, local inner product M is the inverse of transmissibility matrix T. The Darcy's law is discretized based on each of the discrete cell as,

$$\mathbf{Mu} = \mathbf{e}p_i - \boldsymbol{\pi}, \ \mathbf{e} = \left(1, \ldots, T\right)^T, \quad \mathbf{u} = \mathbf{T}\left(\mathbf{e}p_i - \boldsymbol{\pi}\right) \tag{4}$$

π represents the pressure taken at the centre of the faces of each discrete cell whereas p is the pressure taken at the centre of the cell. The flux and pressure drop, when written in tensor notation form,

$$u_k = -n_k \mathbf{K}\mathbf{a}, \quad p_i - \pi_j = c_{ik} \cdot \mathbf{a} \tag{5}$$

Inner product $\mathbf{M}$ and transmissibility matrix $\mathbf{T}$ are related to one another to form a consistency condition necessarily to be obeyed through the calculation,

$$\mathbf{MNK} = \mathbf{C}, \ \mathbf{NK} = \mathbf{TC} \tag{6}$$

Using hybridised mixed form of discretization scheme, we obtain a linear system that describes the continuity of flux and pressure across each cell and face [13].

$$\begin{bmatrix} \mathbf{B} & \mathbf{C} & \mathbf{D} \\ \mathbf{C}^{\mathrm{T}} & 0 & 0 \\ \mathbf{D}^{\mathrm{T}} & 0 & 0 \end{bmatrix} \begin{Bmatrix} u \\ -p \\ \pi \end{Bmatrix} = \begin{Bmatrix} 0 \\ q \\ 0 \end{Bmatrix} \tag{7}$$

In the 3×3 matrix on the left of Eq. 7, row one correspond to Darcy's law; row two is the mass conservation of cells, whereas row three is the continuity of fluxes of all cell faces. To solve the linear system of hybridized discretization method, we use Schur-Complement method and block-wise Gaussian elimination. The application of the methods yield the face pressure as,

$$\left(\mathbf{D}^T\mathbf{B}^{-1}\mathbf{D}-\mathbf{F}^T\mathbf{L}^{-1}\mathbf{F}\right)\boldsymbol{\pi}=\mathbf{F}^T\mathbf{L}^{-1}\mathbf{q} \tag{8}$$

where $\mathbf{F}=\mathbf{C}^T\mathbf{B}^{-1}\mathbf{D}$ and $\mathbf{L}=\mathbf{C}^T\mathbf{B}^{-1}\mathbf{C}$. By solving for face pressures, cell pressures and fluxes can be obtained by back substitution,

$$\mathbf{Lp}=\mathbf{q}+\mathbf{F}\boldsymbol{\pi},\quad \mathbf{Bu}=\mathbf{Cp}-\mathbf{D}\boldsymbol{\pi} \tag{9}$$

The algebraic approximations for the $\mathbf{B}^{-1}$ matrix is obtained from mimetic method.

3 Methodology

Simulations on CO_2 injection into brine solution are implemented using Matlab based on the final form of Eq. 7. Structured Cartesian grid with $60\times60\times5$ dimensions have been set up, as in Fig. 1 to study the effects of capillary pressure, which the properties are listed in Table 1.

Table 1. Saline aquifer's parameters.

Properties	Values
Permeability, *k* (m2)	1.0×10^{-12}
Porosity,	4.5×10^{-10}
Residual CO_2 Saturation	0.25
Residual water saturation	0.30

4 Result and Discussion

The injection well is located in the centre of the x-y plane of the grid generated whereas the production well is located at the far end of the other corner, as shown in Fig. 1. The boundary of the grid is set to be no flow condition. The results with and without capillary pressure are compared and discussed.

Capillary effects will govern the motion of the fluid phase that enters a porous medium initially occupied by the other phase of fluid. The capillary effects is not only accounted by the capillary pressure but also the relative permeability. Referring to Fig. 2, neglecting the capillary force has shown distinctive areas of different CO_2 saturation, with saturation about 1 from the well centre to 0 as the location goes further from the injection well. This means that the propagation of CO_2 in the aquifer is underestimated if we neglect the effect of capillary pressure. This causes distinctive saturation difference along the distance from injection well. Contradictory, when we include the effects of capillary pressure in the flow of CO_2, the saturation of CO_2 within the area of study is about 0.4 to 0.6 after 300 days. From here, capillary pressure will accelerate the migration of CO_2 plume at the early time injection as discussed in [14].

The CO_2 pressure distribution after 300 days of injection show variation when we compare the case with and without capillary effects in Fig 3. The pressure distribution is about the same for both cases but the pattern of distribution varies. Without capillary pressure, a higher pressure distribution is found around the injection well whereas with capillary effect, the reservoir pressure is more evenly distributed throughout the area. There is not much different in the flux intensity of CO_2 after 300 days of injection. In short, capillary pressure affect the saturation and pressure distribution of CO_2 after some time of injection, but it show insignificant effect on flux intensity of CO_2.

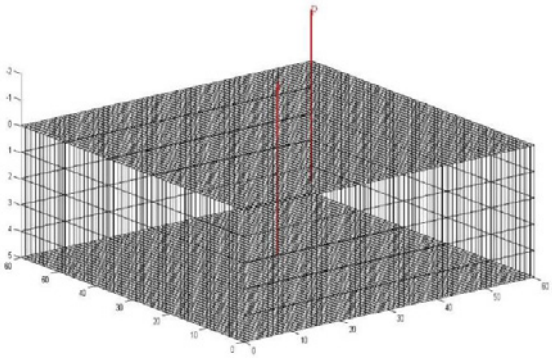

Figure 1. Computational grid with $60 \times 60 \times 5$ dimensions.

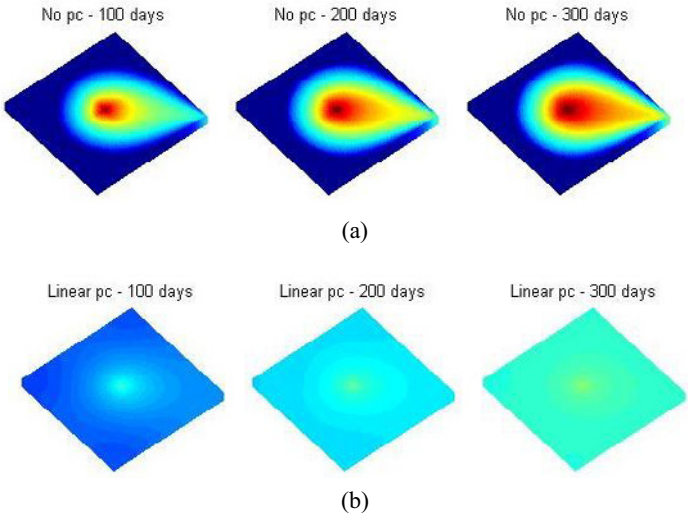

Figure 2. Comparison of CO_2 saturation after 300 days: (a) without P_c and (b) with P_c.

Figure 3. Comparison of pressure distribution after 300 days: (a) without P_c and (b) with P_c.

Figure 4. Comparison of flux of intensity after 300 days: (a) without P_c and (b) with P_c.

5 Conclusion

The study of CO_2 migration in saline aquifer is important as saline aquifer serve as the highest capacity geological storage media for carbon capture and storage (CCS). CCS is identified as one of the promising technology to reduce GHG. In predicting the flow of CO_2 in the saline aquifer, capillary effect significant parameter at the beginning of injection. This research showed that the exclusion of capillary pressure will underestimate CO_2 plume migration. The distribution of CO_2 pressure after 300 days of injection with capillary pressure is more even. However, the effect of capillary pressure on flux intensity of CO_2 is minor. This research can be further enhanced by including the effect of geochemical evolution during CO_2 injection in saline aquifer, particularly the precipitation of salt due to water evaporation.

Acknowledgement

The authors would like to thank UTP EOR MOR for their financial support on this research via YUTP 015-3AA-A65.

References

1. J. Nordbotten, M. Celia and S. Bachu, *Transp. Porous Med.* **70**, 339-360 (2005).
2. U. Goerke, C. Park, W. Wang, A. Singh and O. Kolditz, *Oil and Gas Science and Technology*, **66**(1), 105-118 (2011).
3. Ç. SINAYUÇ, *The Largest Potential Volumes for Geological Storage of CO_2* (2012).
4. IPCC, *Climate Change: The Physical Science Basis. Contribution of Working Group 1 to the Fourth Assessment Report of the Intergovernmental Panel on Climate Change* (Cambridge University Press, 2007).
5. S. Scharf and T. Clemens, *SPE Europe/EAGE Annual Conference and Exhibition* (2006).
6. P. Freund, *Exploration Geophysics*, **37**, 1-9 (2006).
7. H. Herzog, E. Drake and E. Adams, CO_2 Capture, *Reuse and Storage Technologies for Mitigating Global Climate Change* (1977).
8. S. Bachu, D. Bonijoly, J. Bradshaw, R. Burruss, S. Holloway, N.P. Christensen and O.M. Mathiassen, *Int. Jour. of Greenhouse Gas Control*, **1**, 430-443 (2007).
9. N. Stern, *Review on the Economics of Climate Change* (Cambridge University Press, 2006).
10. K. Mosthaf, *CO_2 Storage into Dipped Saline Aquifers Including Ambient Water Flow* (2007).
11. A.F. Gulbransen, V.L. Hauge and K.A. Lie, *SPE Reservoir Simulation Symposium* (2009).
12. F. Brezzi, M. Fortin, *Mixed and Hybrid Finite Element Methods* (Springer, 1991).
13. J.T. Birkholzer, Q.L. Zhou and C.F. Tsang, *Int. Jour. of Greenhouse Gas Control* **3**, 181-194 (2009).
14. I.R. Goumiri, J.H. Prevost and M. Preisig, *Int. J. Num. & Anal. Meth. in Geomechanics* (2011).
15. K.A. Lie, S. Krogstad, I.S. Ligaarden, J.R. Natvig, H.M. Nilsen and B. Skaflestad, *Computer Geoscience*, 297-322 (2012).